LA-UR- 08-5624

Approved for public release; distribution is unlimited.

Title:	The Solvent Dependent Shift of the Amide I Band of a Fully Solvated Peptide in Methanol/Water Mixtures as a Local Probe for the Solvent Composition in the Peptide/Solvent Interface.
Author(s):	S. Gnanakaran, Z # 180405, T-10/T-Divison
Intended for:	Journal: J. Chemistry Physics

Los Alamos
NATIONAL LABORATORY
EST. 1943

Form 836 (7/06)

The Solvent Dependent Shift of the Amide I Band of a Fully Solvated Peptide in Methanol/Water Mixtures as a Local Probe for the Solvent Composition in the Peptide/Solvent Interface

Dietmar Paschek,[1,2,*] Matthias Pühse,[2] Arnold Perez-Goicochea,[2] S. Gnanakaran,[3] Angel E. García,[4] Sean M. Decatur,[5] Alfons Geiger,[2] and Roland Winter[2]

[1] *Lehrstuhl Thermodynamik, Fakultät Bio- und Chemieingenieurwesen, TU Dortmund, Emil-Figge-Str. 70, D-44227 Dortmund, Germany*
[2] *Physikalische Chemie, Fakultät Chemie, TU Dortmund, Otto-Hahn-Str. 6, D-44227 Dortmund, Germany*
[3] *Los Alamos National Laboratory, T10-MS K710, Los Alamos, NM 87545 USA*
[4] *Department of Physics, Applied Physics, and Astronomy, Rensselaer Polytechnic Institute, 110 Eighth Street, Troy, NY 12180-3590 USA*
[5] *Department of Chemistry, Mount Holyoke College, S. Hadley, Massachusetts, 01075 USA*

(Dated: July 14, 2008)

We determine the shift and line-shape of the amide I band of a model AK-peptide from molecular dynamics (MD) simulations of the peptide dissolved in methanol/water mixtures with varying composition. The IR-spectra are determined from a transition dipole coupling exciton model. A simplified empirical model Hamiltonian is employed, taking both the effect of hydrogen bonding, as well as intramolecular vibrational coupling into account. We consider a single isolated AK-peptide in a mostly helical conformation, while the solvent is represented by 2600 methanol or water molecules, simulated for a pressure of 1 bar and a temperature of 300 K. Over the course of the simulations minor reversible conformational changes at the termini are observed, which are found to only slightly affect the calculated spectral properties. Over the entire composition range, varying from pure water to the pure methanol solvent, a monotonous blue-shift of the IR amide I band of about 8 wavenumbers is observed. The shift is found to be caused by two counter-compensating effects: An intramolecular red-shift of about 1.2 wavenumbers, due to stronger intramolecular hydrogen-bonding in a methanol-rich environment. Dominating, however, is the intermolecular solvent-dependent blue-shift of about 10 wavenumbers, being attributed to the less effective hydrogen bond donor capabilities of methanol compared to water. The importance of solvent-contribution to the IR-shift, as well as the significantly different hydrogen formation capabilities of water and methanol make the amide I band sensitive to composition changes in the local environment close the peptide/solvent interface. This allows, in principle, an experimental determination of the composition of the solvent in close proximity to the peptide surface. For the AK-peptide case we observe at low methanol concentrations a significantly enhanced methanol concentration at the peptide/solvent-interface, supposedly promoted by the partially hydrophobic character of the AK-peptide's solvent accessible surface.

INTRODUCTION

Alanine rich peptides have been shown to form stable helices in an aqueous environment [1]. Numerous IR spectroscopic studies have been focusing on the thermodynamics and kinetics of helix formation by probing the temperature induced unfolding transition [1–6]. Recent advances in computer simulation methodology provided the opportunity to study the nature and structural inhomogeneity of helix formation in great detail [7–9]. Simulation data delivered insights by predicting the shift and line shape of the amide I band taking into account both, the effect of hydrogen bonding, as well as intramolecular vibrational coupling [7, 9]. Moreover, the pressure dependence of the amide I band revealed the importance of the solvent contribution to the pressure induced red-shift. The observed solvent induced shift is found to be about three to four times larger than the contribution due to conformational changes of the peptide [9, 10] or the "elastic compression" of the helix. The solvent effect on the IR spectrum has also be observed in pressure studies of poly(N-isopropylacrylamide) in aqueous solution [11], where intramolecular hydrogen bonds play no role. Here we would like to utilize this solvent contribution to the amide I band to study the interaction of the peptide with co-solvents. The effect of co-solvents on the stability of proteins has been attributed to the specific solvent mediated attractive or repulsive interaction of the co-solvent with the protein, leading to a specific excess concentration of the co-solvent in the vicinity of the protein [12–15]. Most of those studies are based on the measurement of excess thermodynamic quantities, which are analyzed in the framework of Kirkwood-Buff theory, assuming concentration changes localized at the protein surface. [15]. In this contribution we focus on the effect of the changing solvent composition on the shift of the amide I band of an 20 amino acid alpha-helical AK-peptide with sequence $Ac-AA(AAKAA)_3AAY-NMe$. In contrast to our previous studies [7, 9], we study solvation changes of the mostly homogeneously folded state of the peptide found at low temperatures. Given that

conformational state of the peptide is only little affected, we suggest that one may employ the solvent dependent shift of the amide I band to determine the local composition of the solvent in the vicinity of the peptide. Based on computer simulations of a realistic model system and from theoretically predicted IR spectra, we show that the water excess concentration in the vicinity of the peptide in a methanol/water mixture can be recovered from the location of the IR-band with reasonable degree of accuracy. We would like to emphasize that complementary experimental techniques such as CD-spectroscopy have to be employed to make sure that the experimentally observed IR shifts are dominated by the changing solvent and only affected to a minor degree by alterations of conformational ensemble of the peptide itself.

METHODS

MD simulation details

We perform MD simulations of a single AK-peptide molecule in methanol/water mixtures with compositions indicated in Table I. Each simulated system contains 2600 solvent molecules in a cubic box with periodic boundary conditions. Water is represented by the three center TIP3P model [16], whereas methanol is described using the TraPPE united-atom forcefield [17, 18]. For the AK-Peptide we employ the AMBER-94 forcefield [19] as modified by García and Sanbonmatsu [20, 21].

We employ molecular dynamics (MD) simulations in the NPT ensemble using the Nosé-Hoover thermostat at $T = 300\,\mathrm{K}$ [22, 23] and the Rahman-Parrinello barostat [24, 25] with coupling times $\tau_T = 1.5\,\mathrm{ps}$ and $\tau_p = 2.5\,\mathrm{ps}$ assuming the isothermal compressibility to be $\chi_T = 4.5\ 10^{-5}\,\mathrm{bar}^{-1}$), respectively. The electrostatic interactions are treated in the "full potential" approach by the smooth particle mesh Ewald summation [26] with a real space cutoff of 0.9 nm and a mesh spacing of approximately 0.12 nm and 4th order interpolation. The Ewald convergence factor α was set to $3.38\,\mathrm{nm}^{-1}$ (corresponding to a relative accuracy of the Ewald sum of 10^{-5}). A 2.0 fs timestep was used for all simulations and the water constraints were solved using the SETTLE procedure [27], while the SHAKE method was used to constrain the bond lengths [28] in methanol and the AK-peptide. All bond-length were kept fixed. All simulations reported here were carried out using the GROMACS 3.2 program [29, 30]. The MOSCITO suite of programs [31] has been employed to generate appropriate start configurations, topology files, and was used for the entire data analysis presented in this paper. The AK-peptide was inserted into the mixture in its full helical state and it was made sure that it stayed in this state during the initial equilibration period. Production runs of 40 ns length were analyzed for each composition. Statistical errors in the analysis were computed using the method of Flyvbjerg and Petersen [32]. For all reported systems initial equilibration runs of 1 ns length were performed using the Berendsen weak coupling scheme for pressure and temperature control ($\tau_T = \tau_p = 0.5\,\mathrm{ps}$) [33].

TABLE I: Parameters characterizing the performed MD-simulation runs. All simulations were carried out at $T = 300\,\mathrm{K}$ and $P = 1\,\mathrm{bar}$. Each simulation contained exactly 2600 solvent molecules plus one helical 20 residue AK-peptide with sequence $\mathrm{Ac} - \mathrm{AA(AAKAA)_3AAY} - \mathrm{NMe}$.

x_{MeOH}	run length τ / ns	Density $\langle\rho\rangle$ / kg m^{-3}
0.0	40	992.39 ± 0.04
0.02	40	985.24 ± 0.03
0.05	40	974.91 ± 0.03
0.1	40	958.95 ± 0.03
0.2	40	930.37 ± 0.04
0.5	40	864.15 ± 0.03
1.0	40	787.61 ± 0.05

Calculation of IR spectra

We use an empirical transition dipole coupling model [34–36] to simulate the trends associated with the amide I band occurring due to both, solvation changes, as well as structural relaxation of the AK-peptide. It was assumed that the amide I manifold states can be separated from all other vibrational modes. The transition dipole coupling modified the nearly degenerate amide I modes and contributes to the off-diagonal terms of an exciton Hamiltonian matrix in the basis of these modes. These matrix elements can be approximated by the transition-dipole-transition-dipole-term

$$\beta_{km} = \frac{\vec{\mu}_k \cdot \vec{\mu}_m - 3\,(\vec{\eta}_{km} \cdot \vec{\mu}_k)\,(\vec{\eta}_{km} \cdot \vec{\mu}_m)}{r_{km}^3}\,, \qquad (1)$$

where $\vec{\mu}_k$ is the effective transition dipole of the kth amide I mode, $\vec{\eta}_{km}$ is the unit vector connecting the dipoles k and m, and r_{km} is the distance between the dipoles [34]. The empirical transition dipole moment has a magnitude of 0.305 D and is located 0.868 Å from the carbonyl carbon along the CO-bond, directed 20° from the CO-bond toward O → N [37]. The application of this empirical model must be cautioned since the nearest neighbor interaction may not be properly represented [38]

The diagonal matrix elements of the Hamiltonian are sensitive to the amide I frequency shifts caused by coupling to other modes and to the solvent. The contribution to the amide I frequency fluctuations from hydrogen bonding interactions between the peptide C=O and

hydrogen bond donors were considered explicitly. Additional amide I frequency shifts dictated by fluctuations in geometry were neglected in our calculations. Frequency shifts due to hydrogen bonding interactions were described in terms of geometrical considerations of the solvent molecules or internal atoms, which are suitably located to perform a hydrogen bond to the C=O-group [39, 40]. We define a hydrogen bond as existing when the distance between the hydrogen of a donor and the oxygen of the peptide unit is less than the hydrogen bond cutoff-distance 2.6 Å and makes favorable angles ($C=O\cdots H$ and $O\cdots H{-}X > 90°$). When these constraints are satisfied, the diagonal shift in frequency $\delta\nu_H$ due to hydrogen bonding (in units of cm^{-1}) is given as:

$$\delta\nu_H = D_H\,(r_{OH} - r^c_{OH}) \qquad (2)$$

with $r^c_{OH} = 2.6$ Å and $D_H = 30\,cm^{-1}Å^{-1}$, and r_{OH} is the $C=O\cdots H-X$ distance given in Å [7, 9, 39–42]. When more than one hydrogen atom satisfied the above criteria, the shift was considered to be additive. For specific hydrogen bonding to carbonyls, the amide I shifts and the additive property are in quantitative agreement with *ab initio* calculations for structures near the equilibrium hydrogen bond distances [43–45]

For each configuration, the Hamiltonian was constructed and diagonalized to obtain the excitonic frequencies and intensities. In the calculation of the amide I spectrum, a separation of time scales between homogeneous and inhomogeneous contributions is assumed. A typical [41] homogeneous dephasing time (T_2) of 0.8 ps has been employed for all investigated solvent compositions, leading to a intrinsic Lorentzian line-shape with 13.2 cm^{-1} FWHM for each of the excitonic frequencies. The ensemble averaging of the frequency spectrum over all configurations obtained from the simulation naturally models the static inhomogeneous contribution to the spectrum and the dephasing describes the motional narrowing in an ad hoc manner. The analysis was carried out for all seven simulations with different solvent compositions. The unperturbed frequency of an amide I oscillator was chosen to be $\nu_0 = 1659\,cm^{-1}$. The specific choice of ν_0 is not critical for our study because the interest is in the change of relative band-shift and shape with respect to the changing solvation conditions.

DISCUSSION

The simulated TIP3P/TraPPE methanol-water model solutions are found to satisfactorily reproduce the thermodynamic and structural properties which are experimentally observed at 300 K and atmospheric pressure. The calculated density variation follows nearly quantitatively the experimental data according to Coquelet et al. [46] (given in Figure 1). The simulations do not

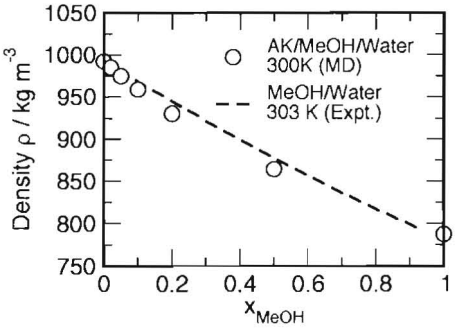

FIG. 1: Experimental densities for binary methanol/water mixtures at $T = 303$ K [46] compared with data from our MD simulations.

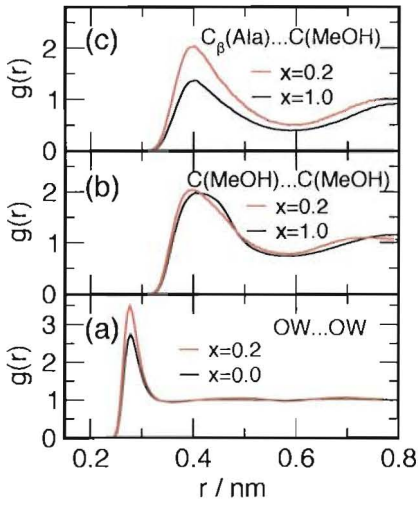

FIG. 2: Comparison of radial distribution functions $g(r)$ (a) Water-water oxgen correlations in pure water and at $x_{MeOH} = 0.2$. (b) methanol-methanol carbon correlations in pure methanol and at $x_{MeOH} = 0.2$. (c) Correlations between methanol carbon and the C_β-atom of the alanine residues of the AK-peptide in pure methanol and at $x_{MeOH} = 0.2$.

show any phase separation tendency, as the calculated radial pair distribution functions, depicted in Figure 2, clearly suggest. Slight systematic deviations of the density are observed at lower concentrations, leading to a somewhat larger slope of the density vs. concentration curve, perhaps indicating a slightly larger partial molar volume of methanol at low concentrations. This observation could hint at a slight overestimation of the tendency of methanol to associate, compared to the real mixture. The first peak features of the calculated radial pair distribution functions shown in Figure 2 are in good agreement with the data obtained from neutron scattering experiments of Dougan et al. [48] and Dixit [49]. A first peak height of the water-water OW-OW pair distribution function increasing from 2.5 at $x_{MeOH} = 0.0$ to about 3.5 $x_{MeOH} = 0.0$ is matches almost exactly the data obtained from empirical potential structure refinement (EPSR) calculations reported in Ref [48], and determined from

TABLE II: Parameters characterizing location of the amide I band, as well as properties characterizing the solvation of the AK-peptide in different methanol water mixtures x_{MeOH}. Here $x_{\mathrm{MeOH}}(\mathrm{local})$ characterizes the composition of the solvent in the vicinity of the peptide. $\langle n_{\mathrm{CO}}(\mathrm{OW})\rangle$ and $\langle n_{\mathrm{CO}}(\mathrm{OH})\rangle$ specify the carbonyl-solvent-oxygen coordination numbers for water (OW) and methanol (OH) as obtained from the corresponding radial distribution functions. ν_{Peak} indicates the peak-position of the calculated amide I band, whereas the $\langle \delta\nu_{\mathrm{intra}}\rangle$ and $\langle \delta\nu_{\mathrm{intra}}\rangle$ represent the relative inter and intramolecular shift-contributions due to the effect of hydrogen bonding.

x_{MeOH}	$x_{\mathrm{MeOH}}(\mathrm{local})$	$\langle n_{\mathrm{CO}}(\mathrm{OH})\rangle$	$\langle n_{\mathrm{CO}}(\mathrm{OW})\rangle$	$\nu_{\mathrm{Peak}}/\mathrm{cm}^{-1}$	$\langle \delta\nu_{\mathrm{intra}}\rangle/\mathrm{cm}^{-1}$	$\langle \delta\nu_{\mathrm{inter}}\rangle/\mathrm{cm}^{-1}$
0.0	0.0	...	1.108	1630.2	-12.93	-15.00
0.02	0.053	0.017	1.020	1631.0	-13.24	-14.07
0.05	0.127	0.040	0.933	1631.7	-13.46	-13.35
0.1	0.234	0.076	0.804	1632.7	-13.31	-12.50
0.2	0.387	0.113	0.630	1633.8	-13.58	-10.76
0.5	0.669	0.197	0.357	1635.7	-13.88	-8.45
1.0	1.0	0.294	...	1638.4	-14.19	-4.92

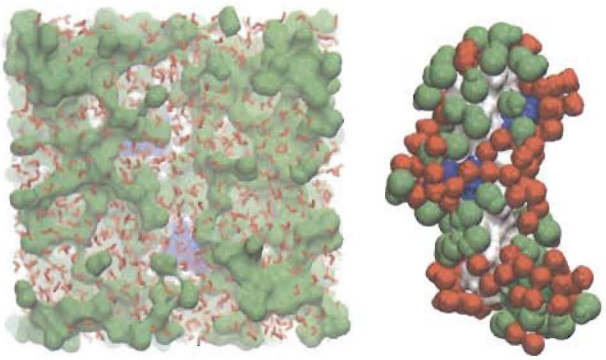

FIG. 3: Pictorial representation [47] of snapshots taken from the simulation with $x_{\mathrm{MeOH}} = 0.2$. Left: Interdigitating networks of methanol and water in the bulk phase (methanol: green; water: red). Right: Shown is the peptides solvent accessible surface, as well as water (red) and methanol (green) molecules in the solvation layer.

neutron scattering data. The observed water-water radial distribution functions, however, are a little less structured compared to what has been reported for methanol-water solutions in Ref. [48], and for the structure of pure water [50, 51]. This has been typically attributed to a underrepresented orientational (tetrahedral) order of neighboring water molecules, being related to the the TIP3P models inability to reproduce waters anomalous thermodynamical features [51, 52]. The almost concentration independence of height of the methanol-methanol carbon peak at a value of about 2 is an additional feature reported in by Dougan et al. [48]. However, the EPSR analysis [48] suggests a slightly decreasing first peak for the mixture, whereas in our simulation the peak height is almost unchanged. Nevertheless, we conclude the simulated mixtures therefore behave on a structural level quite similarly to what has been characterized as a bipercolating mixture by Dougan et al. [48]. The snapshot of a $x_{\mathrm{MeOH}} = 0.2$ mixture shown in Figure 3 illustrates the three-dimensional structural nature of the mixture beyond simple pair-correlations. An analysis based on cluster size distributions of hydrophobic methanol-methanol contacts in the water rich region (not shown) indicates that for small cluster sizes, the distribution of cluster sizes approaches $P(s) \approx s^{-\tau}$ with an exponent of $\tau = 2.18$, where s representing the number of molecules forming a cluster. The same value is observed for the case of random bond percolation on a three-dimensional 3D lattice close to the percolation transition, and is supporting the view of methanol and water as a bi-percolating mixture, as proposed by Dougan et al [48]. The observation of percolation is a feature apparently not untypical for aqueous solutions and has been first observed for the water network in THF/water mixtures by Oleinikova et al. [53], and has been also found later for the hydrophobic clustering of tertiary butanol (TBA) in TBA/water mixtures [54]. Quite interestingly, the broad cluster-size distribution has also implications on the structure of the solvent at peptide solvent interface. As the picture of the solvation shell of the AK-peptide in Figure 3 suggests, the nano-heterogeneous nature is also reflected on the peptide surface and reveals a patchy structure of methanol and water clusters. One may envision a subtle interplay between size and distribution of solvent composition fluctuations at protein surfaces and the possible conformational response of the protein, which seems worth to be further explored in the future.

Figure 2c shows the pair correlation functions between methanol carbons and the methyl sidechains of the Alanine residues. The increase of the first peak at a concentration $x_{\mathrm{MeOH}} = 0.2$ compared to the pure methanol solutions indicates an increasing aggregation of methanol at low concentration, supposedly due to the partial hydrophobic character of the folded Alanine helix. To elu-

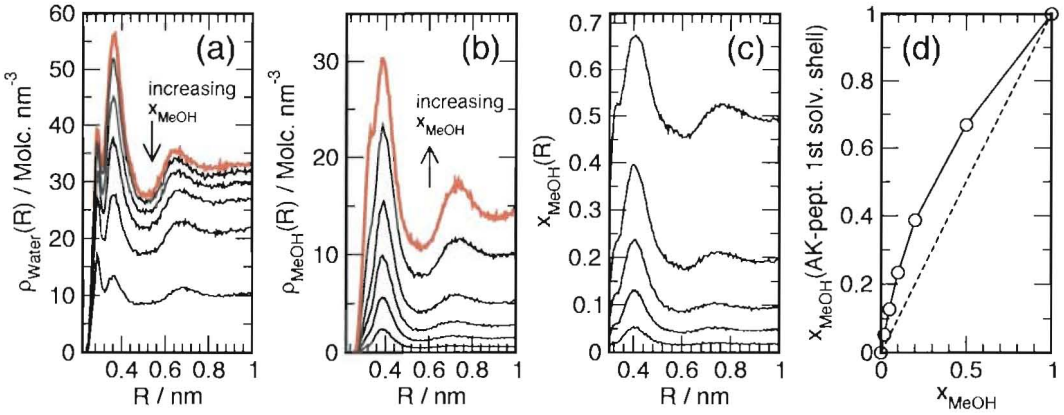

FIG. 4: Solvent densities as obtained by proximal radial distribution functions of water (a) and methanol (b) as a function of distance R normal to the peptide/solvent interface. (c) composition of the solvent as a function of distance from the peptide/solvent interface (d) composition of the solvent in the vicinity ($R \approx 0.4$ nm) of the peptide/solvent interface as a function of solvent composition.

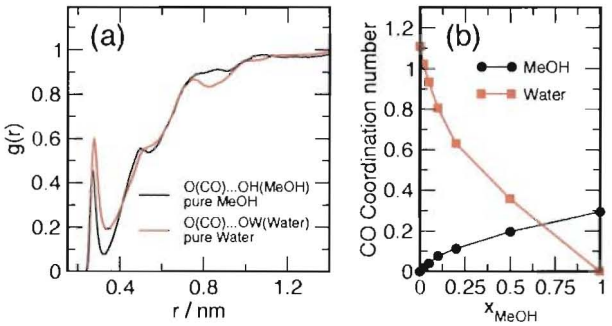

FIG. 5: a) Oxygen-oxygen radial pair distribution function between the oxygen of the amide groups and the water-oxygen in a pure water solvent, as well as the methanol-oxygen in a pure methanol solvent. b) Water and methanol Coordination numbers obtained from the first peak of the O(CO) – OH and O(CO) – OW radial pair distribution functions for all simulated mixtures.

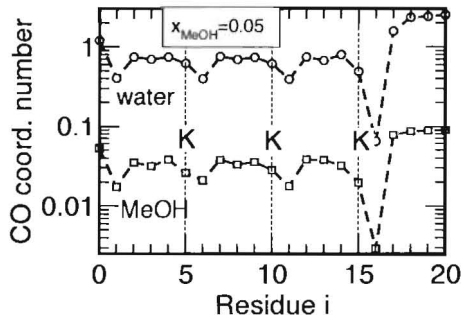

FIG. 6: Water and methanol coordination numbers obtained from the first peak of the O(CO) – OH and O(CO) – OW radial pair distribution functions for $x_{\mathrm{MeOH}} = 0.05$. The given coordination numbers are obtained for each residue individually.

cidate the effect of partial aggregation, we inspect the water and methanol densities in close proximity to the peptide. We use a procedure of calculating peptide-water *proximal pair correlation functions* $g_{\mathrm{prox}}(R)$, similar to Ashbaugh and Paulaitis [55, 56], and also suggested earlier by [57, 58]. As reference sites we use heavy atoms of the peptide (C,N,O) and the center of mass of the solvent molecules. The normalization volume $s(r)dr$ is defined by volume elements with a shortest distance to any atom belonging to the set of peptide heavy atoms. Figure 4ab show the proximal radial distribution function between the peptide and methanol or water. The given $\rho_{\mathrm{prox}}(R)$ for water exhibit a typical two-peak feature, which has been reported to be according to the hydration of polar and nonpolar atoms [58, 59]. Note that the proportion between the two peaks is strongly concentration dependent and is markedly different for the pure liquid than for proteins reported hitherto [58, 59], with the nonpolar peak being apparently significantly more dominant for the AK-peptide. This suggests that the surface of larger size proteins is on average significantly more polar than the surface of the AK-peptide. For the case of methanol shown in Figure 4b the two peaks are largely fused to one. From the densities of the individual components we calculate the local composition as a function of distance to the peptide according to

$$x_{\mathrm{MeOH}}(R) = \frac{\rho_{\mathrm{MeOH}}(R)}{\rho_{\mathrm{MeOH}}(R) + \rho_{\mathrm{Water}}(R)}\,, \qquad (3)$$

shown in Figure 4c. The composition at the peak distance with $R \approx 0.4$ nm indicates a more than twofold enhanced concentration of methanol at the solvation layer in the water rich region. For large distances $R \to \infty$, $x_{\mathrm{MeOH}}(R)$ converges to the composition of the bulk phase. The quantified "local" composition of the mixture at the interface (at $R \approx 0.4$ nm) is given in Figure 4c and Table II. The observed decrease of the $x_{\mathrm{MeOH}}(R)$ for short distances shown in Figure 4c is an artifact based on the fact that we employ center of mass of the molecules as reference, and that the water molecule has a smaller size compared to methanol. The analysis of the composition of the solvation layer is complemented with a detailed description of the solvation of the carbonyl groups of the

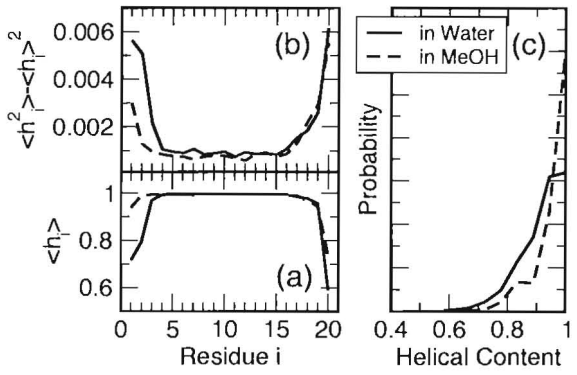

FIG. 7: (a) Probability to find the i'th residue in the alpha-helical state $\langle h_i \rangle$. (b) Fluctuation of the helicity of the individiual residues. (c) Distribution of the helical content of the entire AK-Peptide.

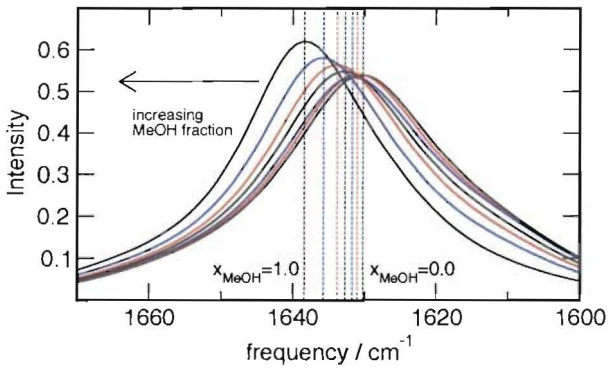

FIG. 8: Calculated IR-spectra for the AK-peptide in methanol/water-mixtures with the compositions: $x_{\mathrm{MeOH}} = \{0.0, 0.02, 0.05, 0.1, 0.2, 0.5, 1.0\}$. The amide I band is found to shift monotonously from $1630.2\,\mathrm{cm}^{-1}$ (pure water) to $1638.4\,\mathrm{cm}^{-1}$ (pure methanol). The vertical lines indicate the peak positions.

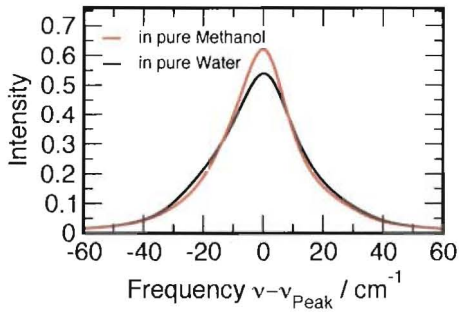

FIG. 9: Calculated amide I bands for the AK-peptide in pure water and methanol shifted relative to their peak-positions ν_{Peak}. Note the increased intensity and narrowed line in a pure methanol solvent.

peptide by calculating the carbonyl oxygen coordination numbers, shown in in Figure 5, and also given in Table II. The coordination number of about 1.1 in pure water is contrasted by an average coordination number of about 0.3 methanol molecules in the pure methanol liquid. Note that the obtained average coordination numbers are found to scale linearly with the "local" composition (compare values given in Table II) of the solvent x^l_{MeOH} according to

$$n_{\mathrm{CO}} = n^*_{\mathrm{CO}}(\mathrm{MeOH}) \times x^l_{\mathrm{MeOH}} + n^*_{\mathrm{CO}}(\mathrm{Water}) \times [1 - x^l_{\mathrm{MeOH}}] \,. \quad (4)$$

The asterisk indicates the coordination number found in the pure solvent. In previous studies it has been shown that side-chain shielding leads to a stabilization of solvated alpha-helical peptide [7, 20, 60]. For the AK-peptide a residue-position dependent alteration of the carbonyl hydration has been reported [7]. For low methanol concentrations a similar behavior is observed here, as the decreased coordination number of the carbonyl-groups of Lysine- (at position i) and the neighboring Alanine-residue (at position $i-4$) indicate. Moreover, in line with the observations reported in Ref. [7], the residues close the C-terminus also show strongly enhanced coordination numbers. As Figure 6 reveals, the methanol solvent exhibits the same coordination pattern as water, however, on a smaller scale. We would like to emphasize that this kind of alternating pattern is only observed in the water rich region and is fully absent in the pure methanol solvent. It is apparently critically related to the hydration pattern of the backbone [20]. The large coordination number of the C-terminal residues is related to enhanced structural fluctuations observed at the termini and has been reported previously [7].

Figure 7 decribes the structural homogeneity of the simulated peptides in terms of it's helical character. The helical content of the AK-peptide is calculated according to the Lifson-Roig definition, which requires three consecutive residues to be helical [61]. Similarly to Refs. [7, 8] the helical state of residue i, is characterized, when (ϕ, ψ) angle lie in the α-helical region of the Ramachandran map $(\phi, \psi) = (-65 \pm 35, -37 \pm 30)$. The helicity $h_i = 1$, in case $(\phi, \psi)_i$ are in the helical region, and $h_i = 0$ otherwise. The averages $\langle h_i \rangle$ characterize the fraction of being in a helical state, and the $\langle h_i^2 \rangle - \langle h_i \rangle^2$ indicate fluctuations of the helicity. Figure 7ab indicate that the molecule is water and methanol solvents predominantly helical, with small conformational alterations restricted to the terminal residues. The methanol solvent seems to stabilize the helical state for the terminal residues. Moreover, it does not only suppress the fluctuations at the termini, but it seems also to affect the conformational fluctuations of the middle residue around their alpha-helical equilibrium, as indicated by Figure 7b. The distribution of the helical content of the AK-petide, given in Figure 7c is accordingly found to be shifted to slightly larger values. The average helical content increases from 0.92 (in water) to 0.96 (in methanol). Although the observed values reveal a strongly homogeneous helical structure of the peptide, they are compatible with data from REMD simulations of the AK-peptide, where a value of about 0.9 was reported for the lowest temperatures [7]. However,

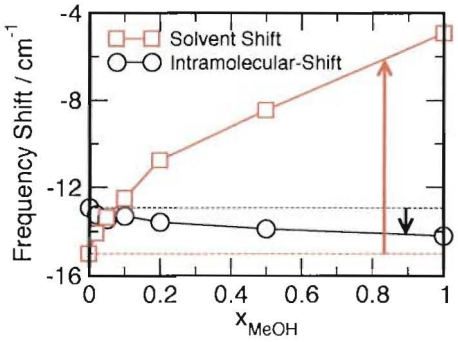

FIG. 10: Inter- and intramolecular hydrogen bond contributions to the shift of amide I band as a function of mixture compositions. The interaction with the solvent leads to a blue-shift of about 10 wavenumbers, which is compensated by a red-shift due to intramolecular hydrogen bonding of about 1.2 wavenumbers.

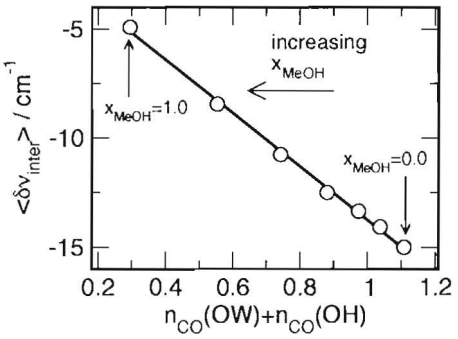

FIG. 11: Correlation between the total coordination number (mehhanol plus water) and the calculated shift of the amide I band due to intermolecular hydrogen bonding.

we cannot fully rule out a small bias towards the helical state due to the limited time window of our simulations. In addition we would like to emphasize that the experimental data of Decatur [62] suggest that the simulated peptide is structurally too homogenously helical.

In the final section of the paper we would like to discuss the calculated spectral properties with changing solvent conditions predicted for the amide I band. Figure 8 shows the calculated amide I bands for all solvent compositions, the peak-frequencies are also given in Table II. We observe a shift of the peak of amide I band of about 8 wavenumbers to larger frequencies, which is quite similar to the shift associated with the helix-coil transition [4]. In the present case, however, the observed shift is apparently mostly due to the changing environment. In contrast to the behavior related the helix-coil transition, the peak intensity does significantly increase and the line-shape is slightly narrowing. Both features are apparently related to the increasing (helical) structural homogeneity, observed for the peptide in a methanol environment. To separate intramolecular from solvent contributions, we have calculated the averages of the solvent shift contributions $\langle \delta\nu_{\rm H} \rangle$ before

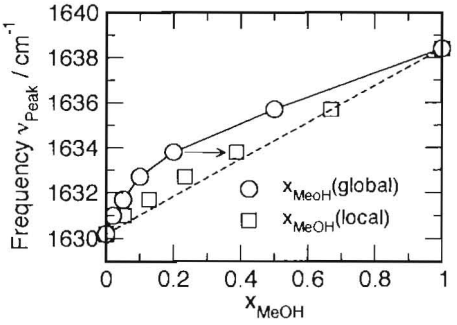

FIG. 12: Location of the peak-position of the amide I band as a function the mixture composition. Here $x_{\rm MeOH}$(global) indicates the composition of the entire solvent, wereas $x_{\rm MeOH}$(local) spcifies the composition of the solvent in the vicinity of the peptide.

employing excitonic mixing. The individual shift components are shown in Figure 10 and also given in Table II. The different contributions are found to have counter-compensating tendency. The intramolecular contribution leads to a red-shift of about 1.2 wavenumbers, apparently due to the more homogenous helical structure and more stable intramolecular hydrogen-bonding. The solvent-contribution, however, leads to a significant blue-shift of about 10 wavenumbers, about one order of magnitude larger than the intramolecular contribution. We conclude that for a case, where the conformational equilibrium of a peptide is only little affected, the solvent contribution to the shift can be the dominating contribution to the shift of the amide I band. This finding is qualitatively in line with the study of Starzyk et al. [63], who observed a blue-shift of the amide I' band of the helical peptide in trifluoroethanol-water-mixtures, while CD-spectroscopy indicated and enhanced helical order. Note that the frequency shift does not change linearly with the composition of the solvent. A significantly increased slope of $\langle \delta\nu_{\rm H} \rangle$ vs. $x_{\rm MeOH}$ is observed in the water-rich region, running parallel with a nonlinearly changing coordination number of the carboxyl-group, given in Figure 5, as well as the enhanced aggregation of methanol in the solvation layer of the AK-peptide described in Figure 4d. Figure 11 suggests that the solvent-contribution to the shift of the amide I band is linearly related to the average total coordination number of the carbonyl groups. This linear dependence and the relation between the coordination number $n_{\rm CO}$ and the *local* solvent composition $x^l_{\rm MeOH}$ given in Eq. 4, suggests that the solvent-contribution to the shift is linearly related to the *local* solvent composition

$$\begin{aligned} \langle \delta\nu_{\rm inter} \rangle &\propto n_{\rm CO} \\ &\propto [n^*_{\rm CO}({\rm MeOH}) - n^*_{\rm CO}({\rm Water})] \times x^l_{\rm MeOH} \\ &\quad + n^*_{\rm CO}({\rm Water})\,. \end{aligned} \tag{5}$$

The location of the peak-position of the amide I bas as a function of solvent composition shown in Figure

12 indicates that this feature is rather well preserved when including intramolecular contributions and even after excitonic mixing. The observed peak-frequencies are a strongly nonlinear function of the mixture composition x_{MeOH}. However, they fall almost completely on the line connecting the peak-positions of the pure liquids when the local compositions x^l_{MeOH} are used instead.

To summarize, although the shift of the peak is in the same range as observed for the temperature induced helix-coil transition, the peak features such as peak-height and peak-width might be used to distinguish it from the helix-coil transition. For the case of a very homogenous solvent insensitive conformational distribution of the peptide th peak-shift is largely dominated by solvent-contributions and is sensitive to the local composition of the solvent. A detailed analysis of the peak-shift might be used to determine the local composition of the solvent in the vicinity of the peptide.

SUMMARY

We have determined the shift and line-shape of the amide I band of a model AK-peptide from molecular dynamics (MD) simulations of the peptide dissolved in methanol/water mixtures with varying composition. The structural features of the simulated methanol/water mixtures are found to be in reasonable agreement with neutron scattering data and show a patchy "bipercolating" clustering structure with a broad cluster-size distribution. For the AK-peptide case we observe at low methanol concentration a significantly enhanced (more than twofold) methanol concentration at the interface, supposedly due to the partially hydrophobic character of the AK-peptide's solvent accessible surface. The patchy structure of the liquid is also observed at the peptide surface. IR-spectroscopic properties are determined from a transition dipole coupling exciton model. A simplified empirical model Hamiltonian is employed, taking both the effect of hydrogen bonding, as well as intramolecular vibrational coupling into account. We consider a single isolated AK-peptide in the mostly folded state, while the solvent is represented by 2600 methanol or water molecules, simulated for a pressure of 1 bar and a temperature of 300 K. Over the course of the simulations minor reversible conformational changes at the termini are observed, which are found to not significantly affect the calculated properties. Over the entire composition range, varying from pure water to the pure methanol solvent, a monotonous nonlinear blue-shift of the IR amide I band of about 8 wavenumbers is observed. The shift of the peak is in the same range as observed for the temperature induced helix-coil transition, however, the peak features such as increasing peak-height and narrowing peak-width might be used to distinguish it from the helix-coil transition. The observed shift is found to be caused by two counter-compensating effects: An intramolecular red-shift of about 1.2 wavenumbers, due to stronger intramolecular hydrogen-bonding in a methanol-rich environment. Dominating, however, is the intermolecular solvent-dependent blue-shift of about 10 wavenumbers, being attributed to the less effective hydrogen bond donor capabilities of methanol compared to water. The importance of solvent-contribution to the IR-shift, as well as the significantly different hydrogen formation capabilities of water and methanol, make the amide I band sensitive to composition changes in the local environment. Moreover, the calculated solvent-shift is found to be linearly related to the (water/methanol) oxygen-coordination number of the carboxyl-groups and to the local methanol concentration. Hence, the composition of the solvent can be determined nearly quantitatively by the measuring the solvent-induced shift of the amide I band. A strongly nonlinear shift of the amide I band with respect to the composition is apparently a good indicator for a significant methanol aggregation at the peptide/solvent interface. This feature could also allow a direct experimental determination of the composition of the solvent in close proximity to the peptide surface.

Acknowledgments AG and RW acknowledge financial support by the Deutsche Forschungsgemeinschaft (FOR436).

---

* Electronic address: dietmar.paschek@udo.edu

[1] S. Marqusee, V. H. Robbins, and R. L. Baldwin, Proc. Natl. Acad. Sci. USA **86**, 5286 (1989).
[2] L. Vila, R. L. Williams, J. A. Grant, J. Woicik, and H. A. Scheraga, Proc. Natl. Acad. Sci. USA **89**, 7821 (1992).
[3] G. Martinez and G. Millhauser, J. Struct. Biol. **114**, 23 (1995).
[4] S. M. Decatur, Acc. Chem. Res. **39**, 169 (2006).
[5] S. M. Decatur and J. Antonic, J. Am. Chem. Soc. **121**, 11914 (1999).
[6] R. A. G. D. Silva, J. Kubelka, P. Bour, S. M. Decatur, and T. A. Keiderling, Proc. Natl. Acad. Sci. USA pp. 8318–8323 (2000).
[7] S. Gnanakaran, R. M. Hochstrasser, and A. E. García, Proc. Natl. Acad. Sci. USA **101**, 9229 (2004).
[8] A. E. García, Polymer **45**, 669 (2004).
[9] D. Paschek, S. Gnanakaran, and A. E. García, Proc. Natl. Acad. Sci. USA **102**, 6765 (2005).
[10] S. M. Decatur, R. Winter, and V. Smirnovas (2008), in preparation.
[11] F. Meersman, J. Wang, Y. Q. Wu, and K. Heremans, Macromolecules **38**, 8923 (2005).
[12] T. Arakawa and S. N. Timasheff, Biochemistry **21**, 6545 (1982).
[13] S. N. Timasheff, Annu. Rev. Biophys. Biomol. Struct. **22**, 67 (1993).
[14] S. N. Timasheff, Adv. Protein Chem. **51**, 355 (1998).
[15] S. Shimizu, Proc. Natl. Acad. Sci. **101**, 1195 (2004).
[16] W. L. Jorgensen, J. Chandrasekhar, J. D. Madura, R. W.

Impey, and M. L. Klein, J. Chem. Phys. **79**, 926 (1983).
[17] M. G. Martin and J. I. Siepmann, J. Phys. Chem. B **102**, 2569 (1998).
[18] B. Chen, J. J. Potoff, and J. I. Siepmann, J. Phys. Chem. B **105**, 3093 (2001).
[19] W. D. Cornell, P. Cieplak, C. I. Bayly, I. R. Gouls, K. M. M. Jr., D. M. Fergueson, D. C. Spellmeyer, T. Fox, J. W. Caldwell, and P. A. Kollman, J. Am. Chem. Soc. **117**, 5179 (1995).
[20] A. E. García and K. Y. Sanbonmatsu, Proc. Natl. Acad. Sci. USA **99**, 2782 (2002).
[21] S. Gnanakaran and A. E. García, J. Phys. Chem. B **107**, 12555 (2003).
[22] S. Nosé, Mol. Phys. **52**, 255 (1984).
[23] W. G. Hoover, Phys. Rev. A **31**, 1695 (1985).
[24] M. Parrinello and A. Rahman, J. Appl. Phys. **52**, 7182 (1981).
[25] S. Nosé and M. L. Klein, Mol. Phys. **50**, 1055 (1983).
[26] U. Essmann, L. Perera, M. L. Berkowitz, T. A. Darden, H. Lee, and L. G. Pedersen, J. Chem. Phys. **103**, 8577 (1995).
[27] S. Miyamoto and P. A. Kollman, J. Comp. Chem. **13**, 952 (1992).
[28] J. P. Ryckaert, G. Ciccotti, and H. J. C. Berendsen, J. Comp. Phys. **23**, 327 (1977).
[29] E. Lindahl, B. Hess, and D. van der Spoel, J. Mol. Model. **7**, 306 (2001).
[30] D. van der Spoel, E. Lindahl, B. Hess, A. R. van Buuren, E. Apol, P. J. Meulenhoff, D. P. Tieleman, A. L. T. M. Sijbers, K. A. Feenstra, R. van Drunen, et al., *Gromacs User Manual version 3.2*, www.gromacs.org (2004).
[31] D. Paschek, *MOSCITO 4 MD simulation package* (2008), http://ganter.chemie.tu-dortmund.de/MOSCITO.
[32] H. Flyvbjerg and H. G. Petersen, J. Chem. Phys. **91**, 461 (1989).
[33] H. J. C. Berendsen, J. P. M. Postma, W. F. van Gunsteren, A. DiNola, and J. R. Haak, J. Chem. Phys. **81**, 3684 (1984).
[34] S. Krimm and J. Bandekar, Adv. Protein Chem. **38**, 181 (1986).
[35] H. Torii and M. Tasumi, J. Chem. Phys. **96**, 3379 (1992).
[36] A. Barth and C. Zscherp, Quart. Rev. Biophys. **35**, 369 (2002).
[37] J. F. Rabolt, W. H. Moore, and S. Krimm, Macromolecules **10**, 1065 (1977).
[38] A. Moran and S. Mukamel, Proc. Natl. Acad. Sci. USA **101**, 506 (2004).
[39] S. Gnanakaran and R. M. Hochstrasser, J. Am. Chem. Soc. **123**, 12886 (2001).
[40] S. Woutersen and P. Hamm, J. Chem. Phys. **115**, 7737 (2001).
[41] P. Hamm, M. H. Lim, and R. M. Hochstrasser, J. Phys. Chem. B **102**, 6123 (1998).
[42] C. Scheurer, A. Piryatinski, and S. Mukamel, J. Am. Chem. Soc. **123**, 3114 (2001).
[43] S. Ham, J. H. Kim, H. Lee, and M. H. Cho, J. Chem. Phys. **118**, 3491 (2003).
[44] H. Torii, T. Tatsumi, and M. Tasumi, J. Raman Spectrosc. **29**, 537 (1998).
[45] H. Torii, T. Tatsumi, and M. Tasumi, J. Phys. Chem. B **102**, 309 (1998).
[46] J. Coquelet, A. Valtz, and D. Richon, J. Chem. Eng. Data **50**, 412 (2005).
[47] W. Humphrey, A. Dalke, and K. Schulten, J. Mol. Grpahics **14**, 33 (1996).
[48] L. Dougan, S. P. Bates, R. Hargreaves, J. P. Fox, J. Crain, J. L. Finney, V. Réat, and A. K. Soper, J. Chem. Phys. **121**, 6456 (2004).
[49] S. Dixit, J. Crain, W. C. K. Poon, J. L. Finney, and A. K. Soper, Nature **416**, 829 (2002).
[50] A. K. Soper, F. Bruni, and M. A. Ricci, J. Chem. Phys. **106**, 247 (1997).
[51] H. W. Horn, W. C. Sope, J. W. Pitera, J. D. Madura, T. J. Dick, G. L. Hura, and T. Head-Gordon, J. Chem. Phys. **120**, 9665 (2004).
[52] D. Paschek, J. Chem. Phys. **120**, 6674 (2004).
[53] A. Oleinikova, I. Brovchenko, A. Geiger, and B. Guillot, J. Chem. Phys. **117**, 3296 (2002).
[54] D. Paschek, A. Geiger, M. J. Hervé, and D. Suter, J. Chem. Phys. **124**, 154508 (2006).
[55] H. S. Ashbaugh and M. E. Paulaitis, J. Phys. Chem. **100**, 1900 (1996).
[56] H. S. Ashbaugh and M. E. Paulaitis, J. Am. Chem. Soc. **123**, 10721 (2001).
[57] P. K. Mehrotra and D. L. Beveridge, J. Am. Chem. Soc. **102**, 4287 (1980).
[58] M. Levitt and R. Sharon, Proc. Natl. Acad. Sci. **85**, 7557 (1988).
[59] N. Smolin and R. Winter, J. Phys. Chem. B **108**, 15928 (2004).
[60] T. Ghosh, S. Garde, and A. E. García, Biophys. J. **85**, 3187 (2003).
[61] S. Lifson and A. Roig, J. Chem. Phys. **34**, 1963 (1961).
[62] S. M. Decatur, Biopolymers **54**, 180 (2000).
[63] A. Starzyk, W. Barber-Armstrong, M. Sridharan, and S. M. Decatur, Biochemistry **44**, 369 (2005).